Pozzo, L.Y.de; Conceicao, T.F.da; Spinelli, A.; Scharnagl, N.; Pires, A.T.N.:
**Chitosan coatings crosslinked with genipin for corrosion protection of AZ31 magnesium alloy sheets**
In: Carbohydrate Polymers (2016) Elsevier

DOI: 10.1016/j.carbpol.2017.10.055

# Chitosan coatings crosslinked with genipin for corrosion protection of magnesium alloys sheet (AZ31)

Ludmila de Y. Pozzo Kiyan [a,*], Thiago F. da Conceição [b], Almir Spinelli [b], Nico Scharnagl [c], Alfredo T. Nunes Pires [b]

[a] Department of materials Engineering, Federal University of Santa Catarina, 88040-900 Florianópolis, SC, Brazil

[b] Department of Chemistry, Federal University of Santa Catarina, 88040-970 Florianópolis, SC, Brazil

[c] Helmholtz-Zentrum Geesthacht GmbH, Institute of Materials Research, Magnesium Innovations Centre - MagIC, Max-Planck-Str. 1, D-21502 Geesthacht, Germany

*e-mail: ludmilapozzo@gmail.com*

**Abstract**

In the present study, coatings of chitosan crosslinked with genipin were prepared on sheets of AZ31 magnesium alloy and their corrosion protection was characterized by means of potentiodynamic polarization and electrochemical impedance spectroscopy (EIS). The coatings were also characterized by means of FTIR, XPS and SEM. It is shown that the crosslinking process decreases the corrosion current and moves the corrosion potential to less negative values. EIS analyzis demonstrate that the crosslinking process increases the maximum impedance at short and long exposure time. The superior performance of the crosslinked coatings is related to a lower swelling degree, as observed in swelling tests for free-standing films.

**Keywords:** Magnesium alloys, chitosan, polymer coating.

## 1. Introduction

The application of polysaccharides as coatings for corrosion protection is an interesting alternative to traditional coatings as these polymers are biodegradable, renewable and soluble in green solvents as water and ethanol. By replacing synthetic resins by polysaccharides it is possible to decrease the emission of volatile organic compounds from the coating industry, as well as its dependency on petroleum derivatives, an important goal for modern society. The literature reports different studies in this context which demonstrate the potential of polysaccharides as corrosion protective coatings (Fekry, Ghoneim, & Ameer, 2014; Heise, Virtanen, & Bocaccini, 2016; Umoren & Eduok, 2016;).

Chitosan is one of the most studied polysaccharides as coatings. Reports in the literature describe the characteristics of chitosan coatings on steels (Umoren et al., 2013; Atta, El-Mahdy, Al-Lohedan, & Ezzat, 2015; John, Joseph, Jose, & Narayana, 2015), aluminium (Zheludkevich et al., 2011; Carneiro et al., 2012), cupper (El-Hadad, 2013) and magnesium alloys (Fekry, Ghoneim, & Ameer, 2014; Mohamed, & Fekry, 2011), among other metals, in which the potential of these coatings is demonstrated. The study of chitosan coatings on magnesium alloys is particularly interesting due to their application as biomaterial, as well as due to their low density which allows the construction of lighter and greener vehicles. Furthermore, magnesium alloys are the engineering metals with the highest tendency for corrosion, a property that has stimulated different studies on corrosion protective coatings (da Conceição & Scharnagl, 2015; da Conceição, Scharnagl, Dietzel, & Kainer, 2012; Gray, & Luan, 2002; Chen et al., 2013; Cui et al., 2013, Pazini et al., 2017; Zhang et al., 2014; Zucchi et al., 2007) .

Chitosan can be crosslinked using different reagents as glutaraldehyde and genipin. From a green-chemistry point of view, genipin is very attractive as it is a natural product, obtained from the fruits of *Gardenia Jasminoides Ellis* and from *Genipina Americana*, and it is biocompatible (Muzzarelli, 2009). Chitosan crosslinked with genipin has received considerable attention in the last years due to its potential application as scaffolds for tissue regeneration (Muzzarelli, Mehtedi, Bottegoni, & Gigante, 2016) and as hydrogels and microcapsules for controlled drug release (Muzzarelli, 2009; Lins, Bazzo, Barreto, & Pires, 2014). The aim of the present study is to explore the potential of chitosan crosslinked with genipin as corrosion protective coatings on a magnesium AZ31

alloy sheet. The effect of different amounts of genipin on the coatings properties is described in details.

## 2. Materials and methods

### *2.1 Materials*

Sheets of AZ31 magnesium alloy, with dimensions of 5.0 x 2.0 x 0.2 cm, were used in this study. The chemical composition of the alloy is shown in Table 1.

Table 1: Chemical composition of the alloy

| Element | Al | Zn | Mn | Si | Cu | Ca | Ni | Fe | Mg |
|---|---|---|---|---|---|---|---|---|---|
| wt.% | 2.97 | 0.85 | 0.24 | 0.02 | <0.01 | <0.01 | <0.01 | 0.03 | Bal. |

Chitosan, with average molar weight ($\bar{M}_n$) of 161,000 g mol$^{-1}$ and degree of deacetylation of 75-85%, sodium hydroxide and acetic acid were obtained from Sigma Aldrich. Genipin (98% of purity) was obtained from Challenge Bioproducts, Taiwan. All chemicals were used without further purification.

### *2.2 Methods*

#### *2.2.1 Preparation of free-standing films*

Chitosan solutions (2.0 wt.%) in acetic acid (0.5 %) were prepare by dissolving the polymer at room temperature. Then, a determined amount of genipin (1, 3 or 6 mmol per mol of chitosan repeat unit), was dissolved under stirring at room temperature for 1 h. Free-standing films were prepared by casting the solutions onto glass plates and let them to dry for 24 h at room temperature. The films were further dried under vacuum at 100 °C for 2 h. The prepared free-standing films are denoted as shown in Table 2.

#### *2.2.2 Coatings preparation*

The applied coating process consisted of two steps: in the first one, a ground sheet (ground using a 1200 grid paper) was immersed in a 2.0 mol L$^{-1}$ NaOH aqueous solution

at 90 °C and under mechanical stirring, for 24 h. Then, the sheet was washed with water and dried under vacuum at 100 °C for 2 h. This pre-treatment was necessary to prevent corrosion of the metal during immersion in the chitosan solution, as it produces a $Mg(OH)_2$ layer on the metal surface. In the second step, the NaOH pre-treated sheets were dip coated with the chitosan solutions described in the previous section. Finally, the coatings were dried at room temperature for 24 h and under vacuum at 100 °C for 3h. The chitosan coatings had a final thickness of 4 – 6 μm as determined by a coating thickness gauge. The samples used in this study are denoted as shown in Table 2.

Table 2: Denotation of the samples used in this study

| Denotation | Description |
|---|---|
| **Free- standing films** | |
| QT | Neat chitosan film |
| QTG1 | Chitosan film with 1 mmol of genipin |
| QTG3 | Chitosan film with 3 mmol of genipin |
| QTG6 | Chitosan film with 6 mmol of genipin |
| **Metallic samples** | |
| AZ31 | As-received sheet |
| AZ31G | Ground sheet |
| AZ31T | Sheet pre-treated with NaOH |
| AZ31Q | Pre-treated sheet coated with chitosan |
| AZ31G1 | AZ31Q with 1 mmol of genipin |
| AZ31G3 | AZ31Q with 3 mmol of genipin |
| AZ31G6 | AZ31Q with 6 mmol of genipin |

*2.2.3 Fourier Transformed Infrared spectroscopy (FTIR)*

Infrared spectra of the coatings were recorded using the spectrophotometer SHIMADZU IRPrestige-21, with the ATR technique (ZnSe prism), in the range of 4000 $cm^{-1}$ to 600 $cm^{-1}$. Each analysis was recorded with 40 scans in a resolution of 4 $cm^{-1}$.

*2.2.4 X-ray photoelectron spectroscopy (XPS)*

X-ray photoelectron spectroscopy (XPS) was performed by using a Kratos DLD Ultra Spectrometer with an Al-Kα X-ray source (monochromator) as anode with power of 225W. The samples were used as received without any further surface preparation or cleaning. For the survey spectra, a pass-energy (PE) of 160 eV was used while for the region scans PE was 40 eV. Charge neutralization was applied during all measurements. Data evaluation was done by using CasaXPS Software. The spectra were calibrated to binding energy of 284.5 eV for C-C of the C1s signal.

*2.2.5 Electrochemical analysis*

Electrochemical Impedance Spectroscopy (EIS) and Potenciodinamic Polarization analyses were performed on a potentiostat PalmSens 3, using a three electrode cell (sample as the working electrode, a graphite rod as auxiliary electrode and Ag/AgCl (saturated) as reference electrode) with an area of approximately 1.0 $cm^2$ exposed to a 3.5 wt.% NaCl solution. EIS measurements were performed from 100 kHz to 10 mHz with an amplitude of 10 mV in relation to the open circuit potential (OCP). Two measurements were performed for each sample. Prior to each analysis, the OCP was measured for 30 minutes to let the system stabilize. The potentiodynamic polarization was performed using a scanning rate of 0.1 mV $s^{-1}$ from -250 mV to 500 mV in relation to OCP. A current limit was set at 10 mA for each analysis. These analyses were also performed after 30 min of OCP measurements for system stabilization. Four measurements were performed for each sample.

*2.2.6 Determination of the swelling degree (SD)*

Swelling experiments were performed on the free-standing films. Dried films, of weight $W_0$, were immersed in a 3.5 wt.% NaCl aqueous solution at room temperature. At determined times the films were removed from the solution, wiped dried with an absorbent paper, and the weight ($W_s$) determined. The swelling degree at each stage was calculated by equation 1. The obtained results represent the average of three measurements for each film.

$$SD = \left( \frac{W_s - W_0}{W_0} \right) x100 \quad Equation\ 1$$

*2.2.7 Scanning electron microscopy (SEM)*

The morphology of the surface and cross-section of the free-standing films was assessed by scanning electron microscopy, using the microscope JEOL JSM-6390LV. The films were previously gold sputtered and the images were obtained using an accelerating voltage of 8 kV. For the acquisition of the cross-section images, the films were cryogenically broke in liquid nitrogen.

## 3. Results and discussion

*3.1 Coating characterization*

The occurrence of the crosslinking of chitosan with genipin could be observed by the change in the film colour, from pale yellow to deep blue. The blue colour is related to the tertiary amine (Touyama, 1994), formed in the reaction of chitosan with genipin, as shown in Figure 1.

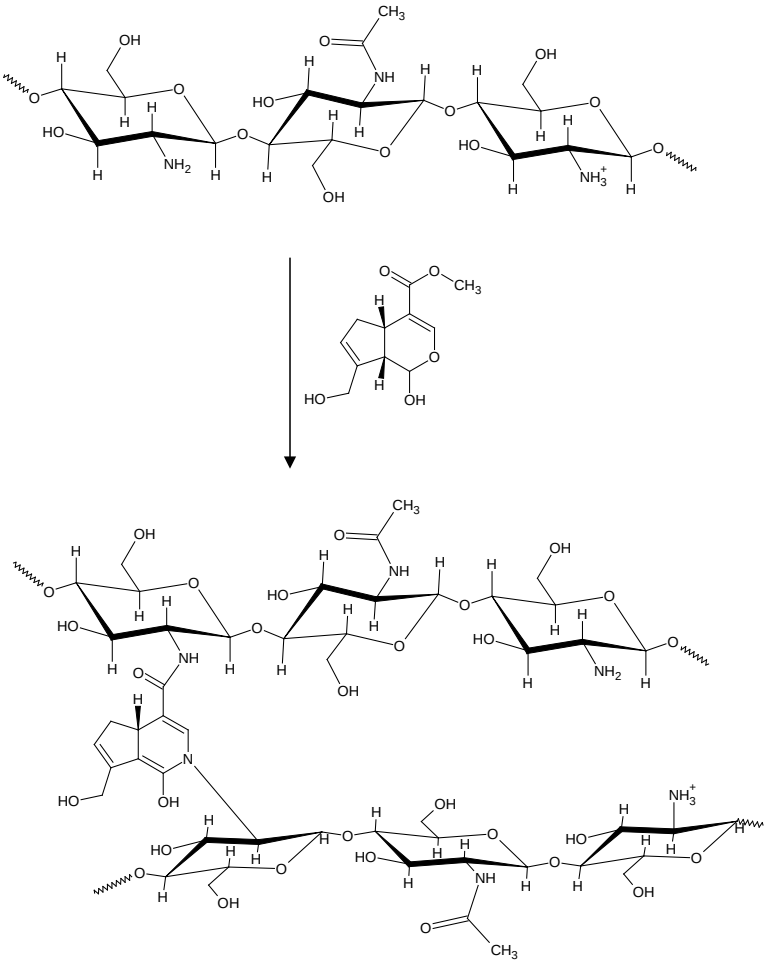

Figure 1: Scheme of the crosslinking reaction of chitosan with genipin.

The FTIR spectra of chitosan films (QT) and chitosan films crosslinked with 6 mmol of genipin (QTG6) are shown in Fig. 2. The spectra show two absorption bands in the range from 1700 $cm^{-1}$ to 1500 $cm^{-1}$, one at 1643 $cm^{-1}$, characteristics of carbonyl stretching mode of amide groups, and at 1546 $cm^{-1}$, related to the bending mode of primary amine and to protonated amine (Lambert, 1987). For QT, the band at 1643 $cm^{-1}$ is related to acetylated units, whereas for QTG6 it is related to acetylated units and to the amide group formed by the reaction of chitosan with genipin (Fig. 1). The reaction of chitosan with genipin is confirmed by an increase in the ratio of the amide and amine absorption bands height ( $h_{1643}/h_{1546}$) for QTG6, in comparison to QT (0.9 for QTG6 and

0.4 for QT). In the spectrum of QTG6 the band at 1319 $cm^{-1}$ is related to the tertiary amine shown in Fig. 1, indicating the occurrence of crosslinking.

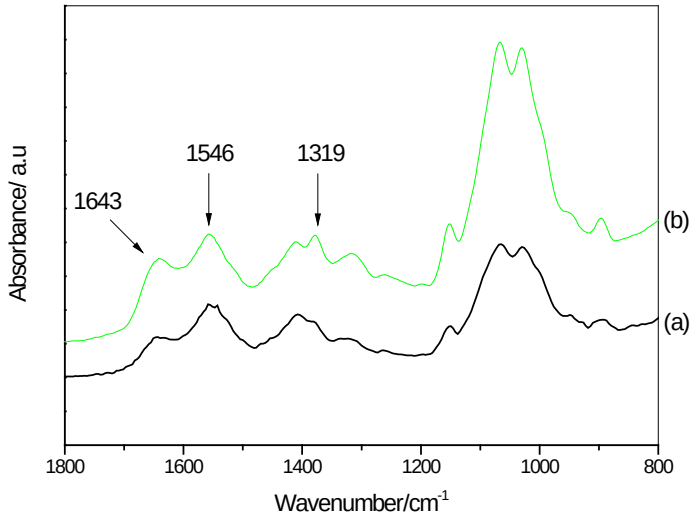


Figure 2: FTIR spectra of QT (a) and QTG6 (b)

XPS analyses corroborate with the FTIR results. Before and after the crosslinking, the N 1s spectra for QT, QTG1 and QTG6 show two convoluted peaks (Fig. 3). The one at 399.5 eV is related to amine (primary and tertiary) and amide groups, and the other, at 400.8 eV, is related to protonated amine ($-NH_3^+$) (Jolm et al., 1992). It can be observed that an increase in the concentration of genipin increases the $h_{400.8}/h_{399.5}$ ratio, in which "h" means the height at the respective binding energy. This result can be explained by the reaction of the amine groups of chitosan with genipin, resulting in the formation of amide and tertiary amine (Fig. 1). The XPS results corroborate with the FTIR ones and confirm the occurrence of crosslinking.

**Kommentiert [NSch1]:** Do not use "height" as a parameter. For XPS the area of the signal is specific!

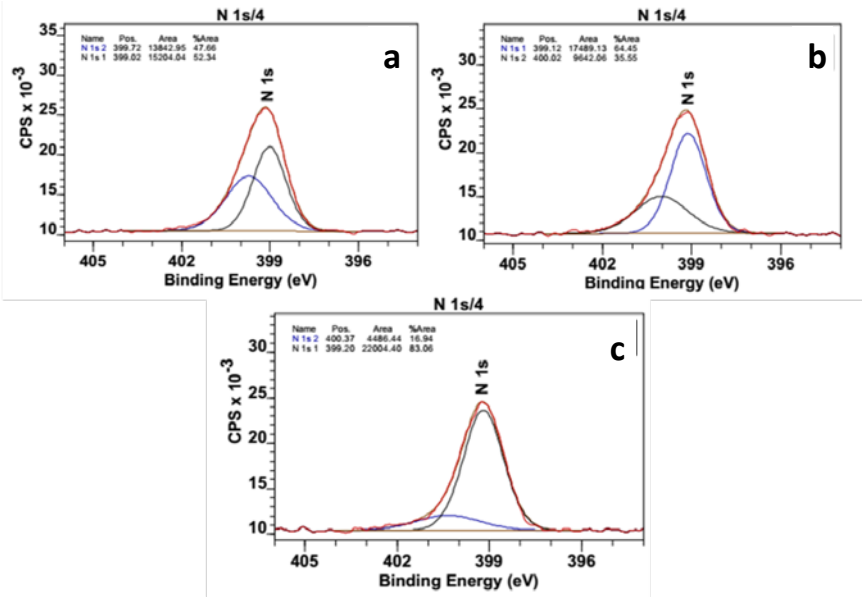


Figure 3: XPS spectra of the N 1s region for: a) QT, b) QTG1 and c) QTG6

*3.2 Electrochemical characterization*

Fig. 4 shows the polarization curves for the analysed samples. It can be observed that AZ31G shows direct metal dissolution immediately above $E_{corr}$ whereas the other samples show lower anodic current. The breakdown potential (in relation to $E_{corr}$) for AZ31T is 127 mV whereas for AZ31 is 43 mV. AZ31Q shows a breakdown potential slightly smaller than AZ31T what may be related to an attack of the acetic acid on the $Mg(OH)_2$ layer of AZ31T. These results show that the treatment of the alloy with NaOH and the coating with chitosan promotes a reduction in the anodic current.

It is interesting to observe that the samples AZ31G1 and AZ31G6 (chitosan with genipin) show the less negative corrosion potential, whereas the other samples show similar values of $E_{corr}$. This result indicates that the crosslinking process reduced the thermodynamic tendency for the alloy oxidation.

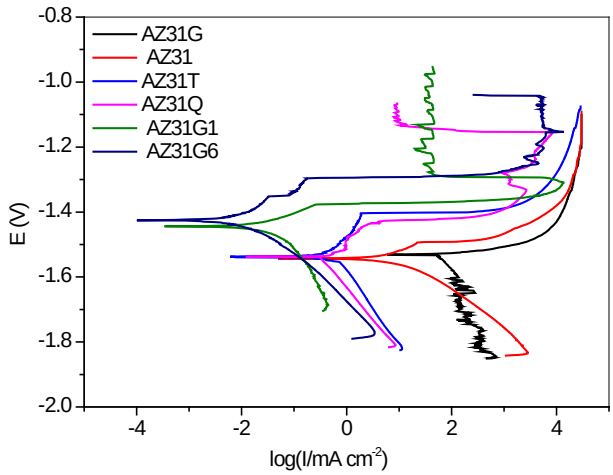


Figure 4: Polarization curves for the samples after 30 min. of exposure to a 3.5 wt.% NaCl aqueous solution.

The corrosion current density ($I_{corr}$) of each sample, obtained using the Tafel method, is shown in Table 3. It can be observed that the sample AZ31T show lower $I_{corr}$ in comparison to AZ31 and AZ31G (nearly 89% of reduction in comparison to AZ31G) indicating that the formed $Mg(OH)_2$ layer improves the corrosion resistance of the alloy.

Table 3: Corrosion potential ($E_{corr}$) and corrosion current density ($I_{corr}$) obtained by the Tafel method for the analysed samples.

| **Samples** | **$E_{corr}$ mV** | **$I_{corr}$ µA/cm²** |
|---|---|---|
| **AZ31** | -1531 ± 6 | 56.9 ± 21.1 |
| **AZ31G** | -1512 ± 82 | 4.27 ± 2.05 |
| **AZ31T** | -1535 ± 17 | 0.69 ± 0.10 |
| **AZ31Q** | -1542 ± 12 | 0.323 ± 0.150 |
| **AZ31G1** | -1440 ± 20 | 0.012 ± 0.005 |
| **AZ31G3** | -1481 ± 25 | 0.049 ± 0.020 |
| **AZ31G6** | -1418 ± 11 | 0.006 ± 0.001 |

It is interesting to observe that there is a significant reduction in $I_{corr}$ with the crosslinking for the chitosan coated samples. A reduction in $I_{corr}$ of approximately 98% is observed for AZ31G6 in comparison to AZ31Q. It can be concluded that the crosslinking of chitosan with genipin resulted in a lower thermodynamic tendency for corrosion (less negative corrosion potential) and a lower corrosion current.

In Fig. 5 it is shown the Bode plot for the analysed samples after one (Fig 5a) and seventeen days (Fig. 5b) of exposure to the corrosive solution. It can be observed that, after one day of exposure, the sample with highest impedance is AZ31G6, followed by AZ31T. The lower impedance of AZ31Q and AZ31G1, in relation to AZ31T, may be due to an attack of the acetic acid on the $Mg(OH)_2$ layer of AZ31T, as mentioned on the discussion of the polarization tests. On the seventh day of exposure, the impedance of AZ31G6 increases to about $10^6$ Ω $cm^2$ whereas the other samples show a decrease in impedance (with the exception of AZ31G, which shown impedance increase due to the deposition of corrosion product on the metal surface). The results show that the crosslinking has a significant effect on the long-term corrosion protection offered by chitosan coatings.

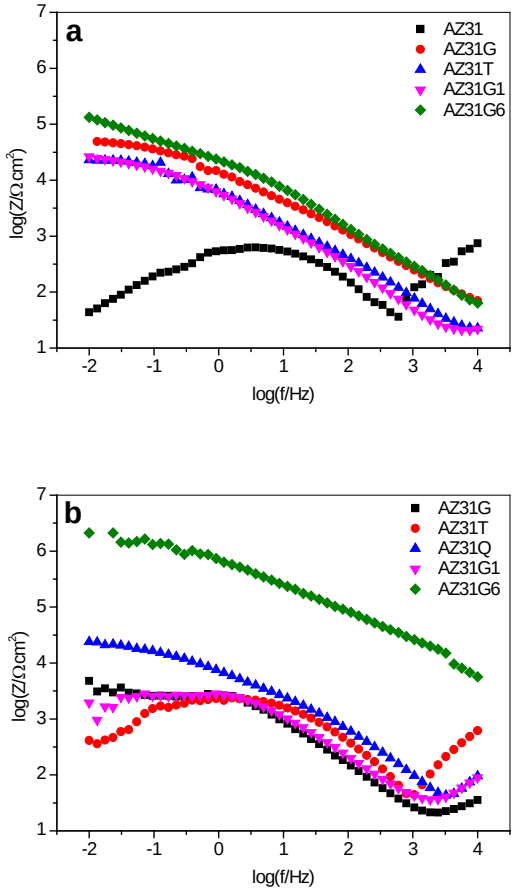


Figure 5: Bode diagram of the samples in the first (a) and the seventh day of exposure (b) to a 3.5 wt.% NaCl aqueous solution

A possible explanation for the superior performance of the coating with higher crosslinking degree is that this sample has a lower water uptake. To confirm this assumption, swelling tests were performed on free-standing films, which were crosslinked in the same manner as the coatings. It can be seen in Fig. 6 that, after 5 h of immersion, the neat chitosan film (QT) has a swelling degree (SD) of 283% whereas QTG6 shows a SD of 176%. This decrease in swelling with crosslinking is related to a decrease in the number of available amine groups and to the lost of chain mobility. It is

interesting to observe that the crosslinking did not changed the kinetics of swelling, as all the films reach the maximum degree of swelling after 10 h of immersion.

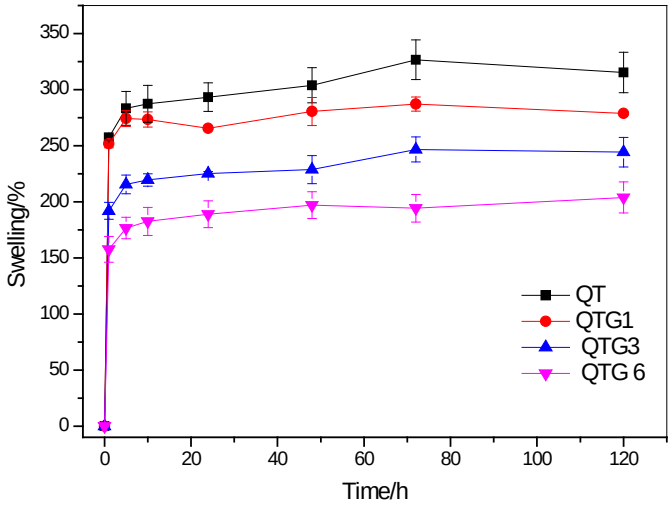


Figure 6: SD of the free-standing films in 3.5 wt.% NaCl aqueous solution.

.

The influence of the swelling on the film morphology was investigated by SEM. Fig. 7a and 7b show the cross-section and surface of QT before swelling, respectively. It can be observed that the film is dense, without pores. After swelling, the cross-section of QT became porous (Fig. 7c). As shown by Figures 7 d-f, the porosity decreases with the increasing of genipin in the films. For QG6 the morphology of the cross-section is very similar to that of QT before swelling. This result corroborates the conclusion that the best corrosion protection observed for AZ31G6 is related to a lower water uptake.

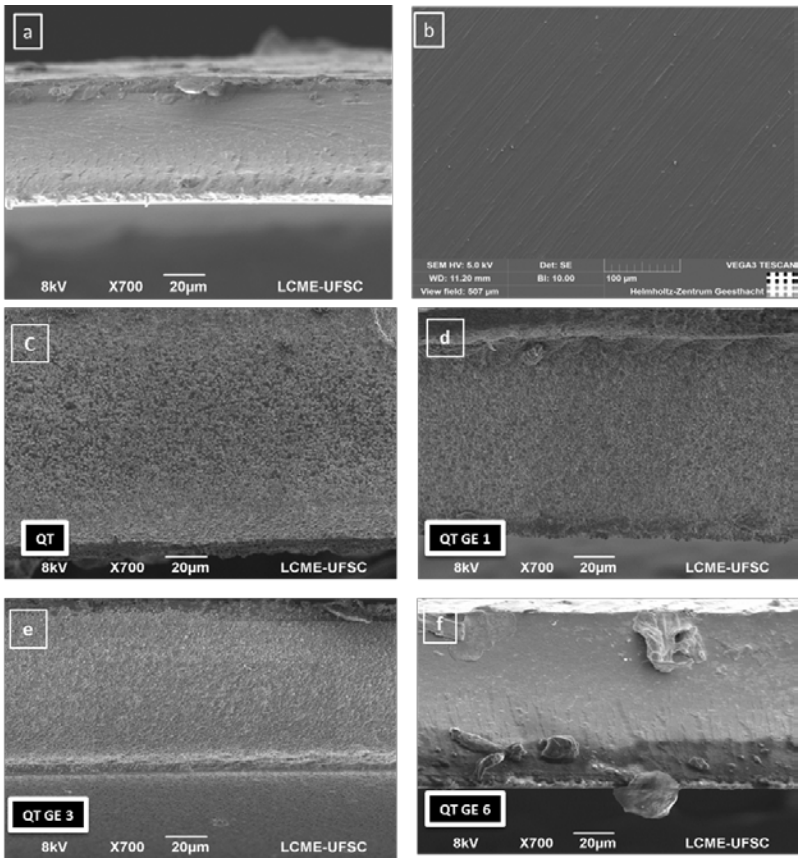


Figure 4: Morphology of the cross-section (a) and surface (b) of QT before swelling. Morphology of the cross-sections of QT (c), QTG1 (d), QTG3 (e) and QTG6 (f) after swelling.

## 4. Conclusion

The crosslinking of chitosan coatings with genipin has a positive influence on the corrosion properties of the coatings. The corrosion current is considerably decreased and the corrosion potential becomes less negative, indicating that the crosslinking process decreases the thermodynamic tendency for corrosion as well as the rate of metal degradation. Tests of electrochemical impedance demonstrate the superior performance of crosslinked coatings in the first and in the seventh day of exposure, indicating superior

long term stability. This superior performance is related to the lower swelling degree of the crosslinked films, as demonstrated in swelling tests.

## 5. References


Atta, A. M., El-Mahdy, G. A., Al-Lohedan, H. A., & Ezzat, A. R. O. (2015). Synthesis ofnonionic amphiphilic chitosan nanoparticles for active corrosion protection ofsteel. *Journal of Molecular Liquids*, *211*, 315–323

da Conceição, T. F., & Scharnagl, N. (2015). Fluoride conversion coatings for magnesium and its alloys for the biological environment. In S. T.S.N., P. I, & L. M. (Eds.), *Surface Modification of Magnesium and Its Alloys for Biomedical Applications* (Vol. 2, pp. 3–21). Cambridge: Woodhead-Publishing. https://doi.org/10.1016/B978-1-78242-078-1.00001-3

da Conceição, T. F., Scharnagl, N., Dietzel, W., & Kainer, K. U. (2012). Controlled degradation of a magnesium alloy in simulated body fluid using hydrofluoric acid treatment followed by polyacrylonitrile coating. *Corrosion Science*, *62*, 83–89. https://doi.org/10.1016/j.corsci.2012.04.041

Boese, E., Èllner, J. G., Heyn, A., Strunz, J., Baierl, C., Schreckenberger, et al. (2001). Kontaktkorrosion einer Magnesiumlegierung mit beschichteten Bauteilen. *Materials and Corrosion*, *52*, 247–256.

Butler, M. F., Ng, Y. F., & Pudney, P. D. A. (2003). Mechanism and kinetics of the crosslinking reaction between biopolymers containing primary amine groups and genipin. *Journal of Polymer Science, Part A: Polymer Chemistry*, *41*, 3941–3953. https://doi.org/10.1002/pola.10960

Cao, F., Song, G. L., & Atrens, A. (2016). Corrosion and passivation of magnesium alloys. *Corrosion Science*, *111*, 835–845. https://doi.org/10.1016/j.corsci.2016.05.041

Carneiro, J., Tedimb, J., Fernandesa, S. C. M., Freire, C. S. R., Silvestre, A. J. D.,Gandinia, A., et al. (2012). Chitosan-based self-healing protective coatingsdoped with cerium nitrate for corrosion protection of aluminum alloy 2024.*Progress in Organic Coatings*, *75*, 8–13.

Chen, J., Song, Y., Shan, D., & Han, E. H. (2012). Study of the in situ growth mechanism of Mg-Al hydrotalcite conversion film on AZ31 magnesium alloy. *Corrosion Science*, *63*, 148–158. https://doi.org/10.1016/j.corsci.2012.05.022

Chen, Y., Luan, B. L., Song, G.-L., Yang, Q., Kingston, D. M., & Bensebaa, F. (2012). An investigation of new barium phosphate chemical conversion coating on AZ31 magnesium alloy. *Surface & Coatings Technology*, *210*, 156–165. https://doi.org/10.1016/j.surfcoat.2012.09.009

Chu, Y. R., & Lin, C. S. (2014). Citrate gel conversion coating on AZ31 magnesium alloys. *Corrosion Science*, *87*, 288–296. https://doi.org/10.1016/j.corsci.2014.06.034

Cui, X. J., Liu, C. H., Yang, R. S., Fu, Q. S., Lin, X. Z., & Gong, M. (2013). Duplex-layered manganese phosphate conversion coating on AZ31 Mg alloy and its initial formation mechanism. *Corrosion Science*, *76*, 474–485. https://doi.org/10.1016/j.corsci.2013.07.024

Dash, M., Chiellini, F., Ottenbrite, R. M., & Chiellini, E. (2011). Chitosan - A versatile semi-synthetic polymer in biomedical applications. *Progress in Polymer Science (Oxford)*, *36*, 981–1014. https://doi.org/10.1016/j.progpolymsci.2011.02.001

El-Haddad, M. N. (2013). Chitosan as a green inhibitor for copper corrosion in acidic medium. *International Journal of Biological Macromolecules*, *55*, 142–149.

Fekry, A. M., Ghoneim, A. A., & Ameer, M. A., (2014). Electrochemical impedance spectroscopy of chitosan coated magnesium alloys in a synthetic sweat medium. *Surface & Coatings Technology*, *238*, 126–132. https://doi.org/10.1016/j.surfcoat.2013.10.058

Gray, J. E., & Luan, B. (2002). Protective coatings on magnesium and its alloys — A critical review. *Journal of Alloys and Compounds*, *336*, 88–113. Retrieved from www.elsevier.com

Heise, S., Virtanen, S., & Boccaccini, A. R. (2016). Tackling Mg alloy corrosion by natural polymer coatings - A review. *Journal of Biomedical Materials Research - Part A*, *104A*(10), 2628–2641. https://doi.org/10.1002/jbm.a.35776

Jian, S. Y., Chu, Y. R., & Lin, C. S. (2015). Permanganate conversion coating on AZ31 magnesium alloys with enhanced corrosion resistance. *Corrosion Science*, *93*, 301–309. https://doi.org/10.1016/j.corsci.2015.01.040

Jin, J., Song, M., & Hourston, D. J. (2004). Novel chitosan-based films cross-linked by genipin with improved physical properties. *Biomacromolecules*, *5*, 162–168. https://doi.org/10.1021/bm034286m

John, S., Joseph, A., Jose, A. J., & Narayana, B. (2015). Enhancement of corrosionprotection of mild steel by chitosan/ZnO nanoparticle composite membranes. *Progress in Organic Coatings*, *84*, 28–34.

Lambert, J. B. (1987). Introduction to organic spectroscopy. New York: Macmillan

Lins, L. C., Bazzo, G. C., Barreto, P. L. M., & Pires, A. T. N. (2014). Composite PHB/Chitosan microparticles obtained by spray drying: Effect of chitosan concentration and crosslinking agents on drug relesase. *Journal of the Brazilian Chemical Society*, *25*(8), 1462–1471. https://doi.org/10.5935/0103-5053.20140129

Mi, F. L., Sung, H. W., & Shyu, S. S. (2001). Release of indomethacin from a novel chitosan microsphere prepared by a naturally occurring crosslinker: Examination of crosslinking and polycation-anionic drug interaction. *Journal of Applied Polymer Science*, *81*, 1700–1711. https://doi.org/10.1002/app.1602

Mohamed, R. R., & Fekry, A. M. (2011). Antimicrobial and anticorrosive activity of adsorbents based on chitosan Schiff's base. *International Journal of Electrochemical Science*, *6*, 2488–2508

Moulder, J. F., Stickle, F. W., Sobol, P. E., Bomben, K. D. (1992). Handbook of X-ray Photoelectron Spectroscopy, Perkin-Elmer Corporation.

Muzzarelli, R. A. A. (2009). Genipin-crosslinked chitosan hydrogels as biomedical and pharmaceutical aids. *Carbohydrate Polymers*, *77*, 1–9. https://doi.org/10.1016/j.carbpol.2009.01.016

Muzzarelli, R. A. A., Mehtedi, M. E., Bottegoni, C., Gigante, A. (2016). Physical properties imparted by genipin to chitosan for tissue regeneration with human stem cells: A review. *International Journal of Biological Macromolecules, 93*, 1366-1381.

Pazini, G. A., da Conceição, T. F., Spinelli, A., Scharnagl, N., Pires, A. T. N.,

Skar, J. I. (1999). Corrosion and corrosion prevention of magnesium alloys* Korrosion und Korrosionsschutz von Magnesiumlegierungen. *Materials and Corrosion*, *50*, 2–6.

Song, G., Hapugoda, S., & St John, D. (2007). Degradation of the surface appearance of magnesium and its alloys in simulated atmospheric environments. *Corrosion Science*, *49*, 1245–1265. https://doi.org/10.1016/j.corsci.2006.07.005

Srinivasan, A., Shin, K. S., & Rajendran, N. (2015). Applications of dynamic electrochemical impedance spectroscopy (DEIS) to evaluate protective coatings formed on AZ31 magnesium alloy. *RSC Advances*, *5*, 29589–29593. https://doi.org/10.1039/c4ra16967k

Sung, H.-W., Chang, Y., Chiu, C.-T., Chen, C.-N., & Liang, H.-C. (1999). Crosslinking characteristics and mechanical properties of a bovine pericardium fixed with a naturally occurring crosslinking agent. *J Biomed Mater Res*, *47*, 116–126.

Touyama, R., Takeda, Y., Inoue, K., Kawamura, I., Yatsuzuka, M., Ikumoto, T., et al. (1994). Studies on the blue pigments produced from genipin and methylamine. I. Structures of the brownish-red pigments, intemediates leading to the blue pigments. *Chemical Pharmaceutical Bulletin (Tokyo)*, *42*, 668–673.

Umoren, S. A., & Eduok, U. M. (2016). Application of carbohydrate polymers as corrosion inhibitors for metal substrates in different media: A review. *Carbohydrate Polymers*, *140*, 314–341. https://doi.org/10.1016/j.carbpol.2015.12.038

Umoren, S. A., Banera, M. J., Garcia, T. A., Gervasi, C. A., & Mırıfico, M. V. (2013).Inhibition of mild steel corrosion in HCl solution using chitosan. *Cellulose, 20*,2529–2545.

Zhang, R., Cai, S., Xu, G., Zhao, H., Li, Y., Wang, X., et al. (2014). Crack self-healing of phytic acid conversion coating on AZ31 magnesium alloy by heat treatment and the corrosion resistance. *Applied Surface Science*, *313*, 896–904. https://doi.org/10.1016/j.apsusc.2014.06.104

Zheludkevich, M. L., Tedim, J., Freire, C. S. R., Fernandes, S. C. M., Kallip, S., Lisenkov, A., et al. (2011). Self-healing protective coatings with “green” chitosan based pre-layer reservoir of corrosion inhibitor. *Journal of Materials Chemistry*, *21*, 4805–4812. https://doi.org/10.1039/c1jm10304k

Zucchi, F., Frignani, A., Grassi, V., Trabanelli, G., & Monticelli, C. (2007). Stannate and permanganate conversion coatings on AZ31 magnesium alloy. *Corrosion Science*, *49*, 4542–4552. https://doi.org/10.1016/j.corsci.2007.04.011